Juergen Schieber, 2013, SEM observations on ion-milled samples of Devonian Black Shales from Indiana and New York: The petrographic context of multiple pore types, *in* W. Camp, E. Diaz, and B. Wawak, eds., Electron microscopy of shale hydrocarbon reservoirs: AAPG Memoir 102, p. 153–171.

13

SEM Observations on Ion-milled Samples of Devonian Black Shales from Indiana and New York: The Petrographic Context of Multiple Pore Types

Juergen Schieber

Indiana University, Department of Geological Sciences, 1001 E. 10th St., Bloomington, Indiana, 47405, U.S.A. (e-mail: jschiebe@indiana.edu)

ABSTRACT

Middle Devonian Marcellus Shale and late Devonian New Albany Shale samples were argon-ion milled and studied by scanning electron microscope for petrographic features and pore development. Petrographic observations revealed that a finite number of pore types exist in spite of considerable variability in composition, depositional setting, and compaction history. The four major pore types are framework pores, framework shelter pores, dissolution pores within inorganic grains, and organic matter pores. Framework pores occur in open spaces of the grain fabric. The most common framework pores are defined by phyllosilicate (clays, micas) and carbonate grains (biogenic, diagenetic) and also occur in areas with abundant diagenetic silica. Framework pores associated with carbonate grains can be well developed where abundant skeletal debris provides shelter porosity. Phyllosilicate framework pores increase in abundance with increasing clay content, but more critically, their abundance in compacted shales hinges on the presence of pressure shadows generated adjacent to mechanically competent grains (quartz, feldspar, dolomite, calcite, pyrite) that resist compaction. Dissolution pores in inorganic grains were predominantly encountered in association with calcite and dolomite grains. In places, other minerals, such as pyrite, also can show dissolution effects, but do not contribute significantly to overall porosity. Dissolution pores probably reflect decreased pH associated with the formation of carboxylic and phenolic acids at elevated temperatures (about 80 to 120° C). At low carbonate contents (a few percent), dissolution pores constitute only isolated porosity, but in shale intervals that contain abundant carbonate, or where carbonate grains were concentrated into laminae, this pore type may be an important facilitator of gas storage and transmission. Pores within organic matter are maturity dependent and restricted to amorphous organic matter (bituminite/amorphinite) in thermally mature samples (>0.6%R_o). Grain and fabric shrinkage during core storage and sample processing produced pore artifacts as well (false pores), and their correct identification is critical for accurate petrographic pore assessment.

DOI: 10.1306/13391711M1023589

INTRODUCTION

Typical shales are sedimentary rocks with a dominant grain size below 63 μm and constitute approximately two-thirds of the sedimentary rock volume (Schieber, 1998). Shales function as the seals that prevent hydrocarbons from escaping from their reservoir, and a subset of carbonaceous (organic-rich) shales serves as source rocks. The first natural gas well in the United States tapped Devonian black shales beneath Fredonia, New York. This well was drilled in 1825, almost four decades before the Drake Oil Well near Titusville, Pennsylvania, which is considered to mark the birth of the oil industry. Though shale gas has been produced in the eastern United States for more than a century, the contribution of shale gas to overall production has been marginal. In the past decade, however, shale gas has become a growing source of natural gas in the United States, spurred by technological advances, such as horizontal drilling and hydraulic fracturing techniques. Increased shale gas production has been essential to offset declining production from conventional gas reservoirs.

Early studies of gas-producing shales focused on Devonian black shales of the eastern United States, strata that have long been known to produce natural gas from fractured as well as nonfractured shale intervals (Broadhead et al., 1982). Petrographic examination of porosity in shales requires electron microscopy. Attempts to produce sufficiently thin and undisturbed samples of shale for transmission electron microscopy (TEM) were long hampered by the difficulties of avoiding mechanical damage inflicted by microtome knives (Davies et al., 1990). The application of argon-ion milling, a sample preparation technique developed by material scientists (Bollinger and Fink, 1980), has helped to overcome this limitation and has enabled imaging of pore spaces and mineral interrelationships at the magnifications needed for shale studies (Jiang et al., 1990; Hover et al., 1996; Rask et al., 1997; Schieber, 1998, 2002). Although shale pores are readily observed in TEM images of argon-ion-milled shales (e.g., Hover et al., 1996), the preferred technique for the study of pores in shales is the scanning electron microscopic (SEM) observation of argon-ion-milled surfaces (Tomutsa et al., 2007; Loucks et al., 2009; Schieber, 2010, 2011). In this study, the focus was on pores that are intrinsic to the shale matrix, although it is acknowledged that fractures can be a significant contributor to the overall porosity of shale intervals.

METHODS

Samples of the Devonian New Albany Shale were collected from a core drilled in Daviess County, Indiana, stored at the core library of the Indiana Geological Survey. Samples of the Devonian Marcellus Shale were provided by Taury Smith of the New York State Museum from a core drilled in northern Chenango County, New York. For location of samples within these wells relative to stratigraphic position and members, see Table 1. Thin slices of these samples were mounted on a custom-designed sample holder and mechanically polished on the top surface. The sample holder was then placed into a GATAN 600 Duomill, and the polished surface was argon-ion milled at a low incident angle for 1 to 3 hours. Milled surfaces were then examined by SEM without conductive coating

Table 1

Well: 1-3 Kavanaugh, Daviess County, Indiana				Well: Beaver Meadow #1, Chenango County, New York			
	Sample	Depth in Meters	Member		Sample	Depth in Meters	Member
Top New Albany Shale		610.11		Top of core		575.5	
	x	612.65	Clegg Creek		x	566.9	Oatka Creek
	x	616.53	Clegg Creek		x	573.9	Oatka Creek
	x	619.88	Clegg Creek		x	582.8	Cherry Valley
	x	622.04	Camp Run		x	588.9	Union Springs
black/gray split	x	623.18	Camp Run	Base Marcellus Shale	x	591.3	Union Springs
	x	634.48	Morgan Trail			592	
	x	637.08	Selmier				
	x	641.02	Selmier				
	x	641.62	Blocher				
	x	644.34	Blocher				
	x	648.85	Blocher				
Base New Albany Shale		649.11					

(FEI Quanta 400 FEG, low-vacuum mode). Our SEM was tested to design specifications just prior to our examination of specimens for this study, and objects of 5 nm size or larger were resolvable. For comparison purposes, a subset of these samples was also polished via edge milling with a GATAN Ilion ion mill. All samples were viewed on surfaces oriented perpendicular to bedding.

Although the ability to make distinctions between organic matter types is critical to the interpretation of the presented research, SEM imaging by itself can only identify organic matter as such based on low backscatter intensities. In this study, the differentiation of amorphous organic matter versus structured organic matter (such as *Tasmanites*) benefited from prior observation of these components in the immature New Albany Shale with fluorescent light microscopy. *Tasmanites*, for example, has an intense yellow fluorescence under UV (ultraviolet) light. In addition, it is a collapsed feature (presence of medial inclusions) of uniform thickness with rounded terminations that shows deformation between harder grains without significant change of thickness. Whereas the UV fluorescence is a matter of chemical composition and fades with maturation, the latter features are morphological in nature and are still readily observed when the sediment has been heated beyond maturity. Given that the New Albany and the Marcellus are both Devonian in age, it can thus safely be assumed that what has the morphology of *Tasmanites* in the mature Marcellus is indeed a collapsed *Tasmanites* cyst.

Amorphous organic matter (bituminite/amorphinite) in the New Albany Shale characteristically is intimately intermingled with mineral matter (clays, silt), shows a dull brownish fluorescence under UV light, is squeezed into interstitial spaces between mineral grains, and lacks any characteristic morphology. The assumption was made that in the mature Marcellus Shale, irregularly shaped and squeezed organic matter with mineral inclusions was the direct equivalent to amorphous organic matter (bituminite/amorphinite) as observed in the New Albany Shale.

Identification of the third organic component considered here, bitumen, is more problematic. In thermally immature rocks, bitumen has not yet evolved, and thus a morphological comparison cannot be made for this component between the New Albany and the Marcellus. The rationale for suggesting a bituminous nature for part of the amorphous organic matter in the Marcellus is the observation of large bubble-like structures of some hundred nanometers in diameter. The bubbles suggest formation in some sort of fluid phase, and the fact that the enclosing organic matter is still in the rock points to a fluid of high viscosity. Thus, one can envision that thermal cracking of bitumen within pore spaces produces gas bubbles within the bitumen. Supporting observations for this view have been reported in a study of maturation effects in the Jurassic Posidonia Shale (Bernard et al., 2012).

NEW ALBANY SHALE

Overview

A 40 m (131 ft) thick core (well 1-3 Kavanaugh, Daviess County) from southern Indiana was examined and sampled (Table 1). The core contains all the stratigraphic subdivisions of the New Albany Shale as

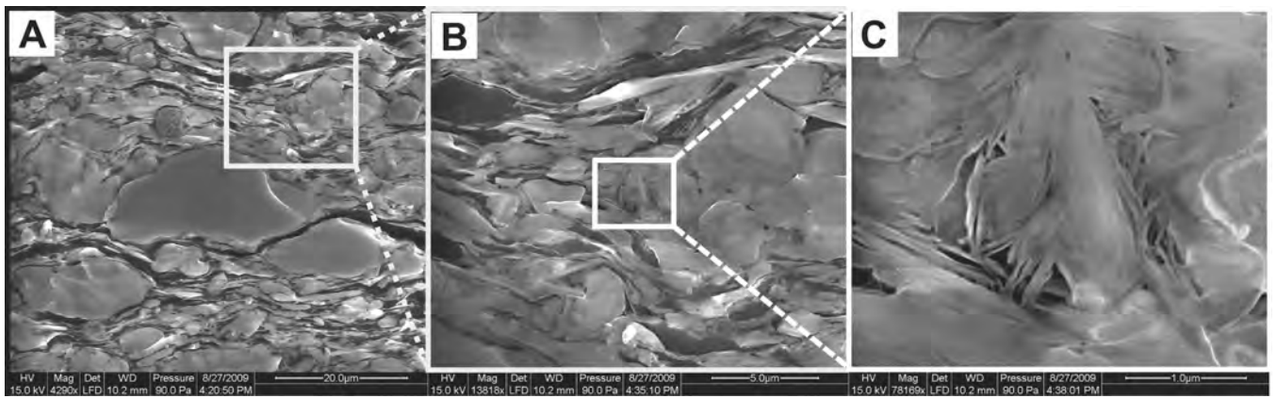

Figure 1. Fabric and phyllosilicate framework pores from the New Albany Shale. (A) Low-magnification secondary electron scanning electron microscopic (SEM) image showing planar fabric caused by compaction and compression around resistant larger grains. Dark streaks consist of kerogen. (B) Enlargement of gray-framed area in (A). Planar-compressed fabric still dominant. (C) Enlargement of white-framed area in (B). Shows largely randomly oriented clays that define triangular openings, here termed phyllosilicate framework pores.

recognized by Lineback (1970). In ascending order, these are the Blocher, Selmier, Morgan Trail, Camp Run, and Clegg Creek members. This core has been studied more recently by Lazar (2007), and a summary of its lithology, sedimentary structures, macrofossils, trace fossils, and total organic carbon content (TOC) was provided by Lazar and Schieber (2004). The 13 samples that were examined include all of the stratigraphic members of the New Albany Shale. The samples include three samples with measured TOC less than 5 wt.%, two samples with TOC values slightly above 5 wt.%, and eight samples with TOC values in excess of 8 wt.%. Measured vitrinite reflectance values indicate that the New Albany Shale in Daviess County is immature (0.57%R_o, Comer et al., 1994).

Observations

Visual estimates from numerous SEM images suggested that framework pores defined by phyllosilicate grains are the most ubiquitous pore type in all New Albany Shale samples. Visual estimates from numerous SEM images suggested that framework pores defined by phyllosilicate grains are the most ubiquitous pore type in all New Albany Shale samples (Figure 1). These pores consist of triangular openings defined by a latticework of randomly oriented clay mineral platelets (Figure 2), ranging in size from 10 nm to more than a micrometer, and occur within a largely compaction-dominated, planar fabric (Figure 2). Phyllosilicate framework pores are best developed in pressure

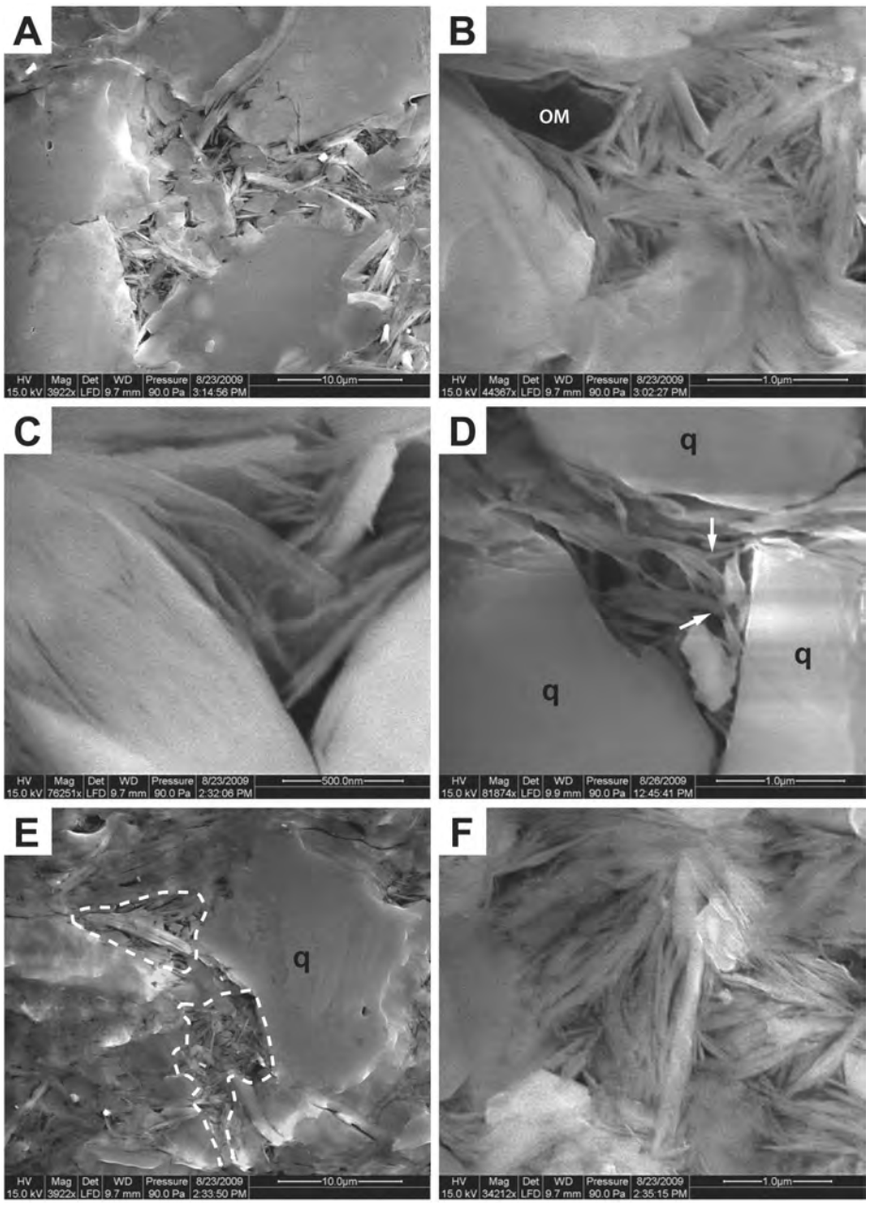

Figure 2. (A) Secondary electron scanning electron microscopic (SEM) images illustrating domains of randomly oriented clay minerals in a silt-rich shale interval of the New Albany Shale. The silt grains provide protection from compaction pressures and allow triangular pores, defined by phyllosilicate platelets, to remain open. (B) Close-up of randomly oriented framework of phyllosilicates with triangular pores. OM marks a piece of probable detrital organic matter. (C) High-magnification image of phyllosilicate framework with triangular pores. (D) Space between small quartz silt grains (q) protects phyllosilicate framework from collapse. Bending of clay flakes (arrows) suggests that at least in part the interstitial clays are of detrital origin. (E) Domains of randomly oriented clay minerals (dashed outlines) with triangular framework pores in pressure shadow of quartz silt grain (q). (F) Close-up of framework texture of randomly oriented phyllosilicates with triangular pores. The central, vertical-oriented clay flake seems to have pierced over and underlying clay flakes because of compaction forces. Images (A) through (F) are from samples that contained approximately 5% total organic carbon (TOC), were rich in quartz silt and clay, and were of medium-to-dark-gray color.

shadows adjacent to larger compaction-resistant grains (rigid grains including fossil debris, silt, and other mineral grains) and in spaces between such grains (Figure 3). In shales, these observed framework pores are analogous to intergranular pores in sandstones. Shales differ from sandstones, however, in that they are generally subject to severe mechanical compaction associated with dewatering during burial. The term framework pore does highlight pore preservation caused by the resistance to compaction by a variety of mineral frameworks.

The pore-defining clay mineral platelets of phyllosilicate framework pores are typically at most a few micrometers in size and appear to have multiple origins. They show textures suggestive of detrital origin, such as bending and splintering caused by compaction, as well as piercing and differential compaction when in near-vertical orientation (Figures 3, 4). Clay minerals that are likely of diagenetic origin tend to be finer grained and more idiomorphic appearing (Hover et al., 1996). They are present in the New Albany Shale but do not appear to be of volumetric importance.

In addition to framework formation by phyllosilicates, early diagenetic growth of carbonate and silicate grains can provide compaction-sheltered spaces that preserve pore space during burial. Figure 5A shows an example of such a pore defined by dolomite grains. Even though the space is now occupied by clay minerals, compaction sheltering by dolomite grains allows open framework pores between clays. In Figure 4B, pore preservation is seen among early diagenetic quartz grains.

In clay-rich shales with low amorphous kerogen content (<5 wt. % TOC) (Figure 3), framework pores appear to remain open through burial history. In contrast, in the samples with more than 5 wt.% TOC, the dispersed amorphous organic matter appears to fill most of the framework pores (Figure 9).

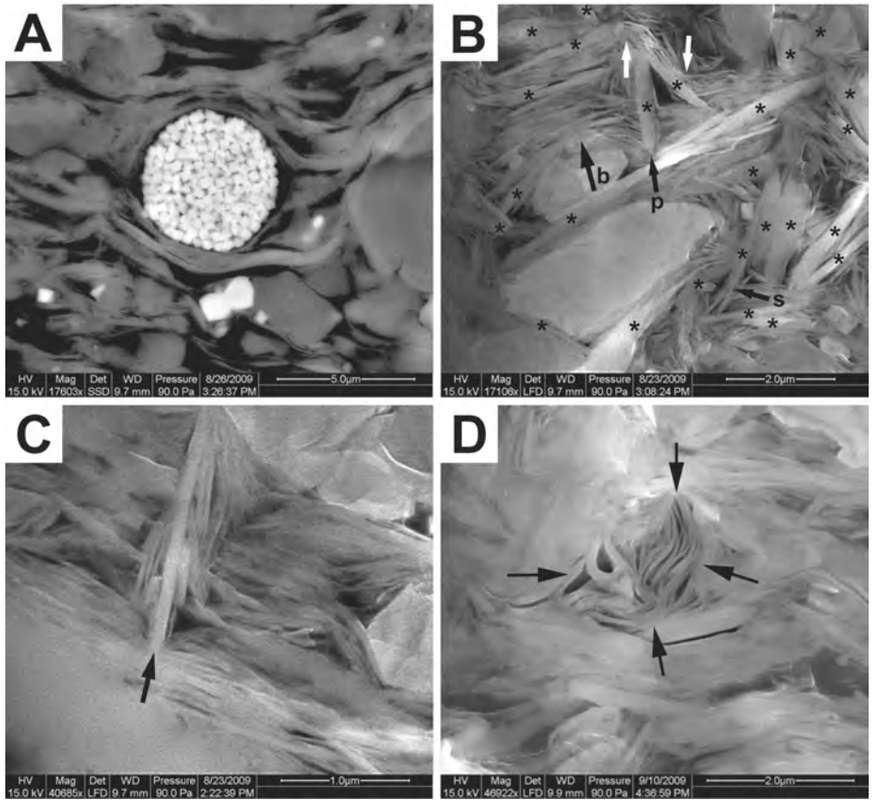

Figure 3. (A) Scanning electron microscopic (SEM) backscattered image that shows bending of detrital clays, mica flakes, and kerogen blebs around pyrite framboid (center) and quartz grains (total organic carbon [TOC] approximately 9%). (B) Random clay fabric with phyllosilicate framework pores. Clay flakes marked with * are considered clearly detrital and define a lattice framework of compaction-protected space. Black arrows: b = compactional bending of clays around quartz grains; s = splintering of clay flake due to compression; and p = piercing by clay flake. White arrows mark wrapping of clays because of compaction. (C) Subvertical clay flake pierces underlying clays because of compaction (black arrow). (D) Black arrows define an area where compression of a vertically oriented phyllosilicate grain produced pores because of splits between phyllosilicate sheets. All images from the New Albany Shale. Images (B)–(D) are secondary electron images; samples contained approximately 5% TOC.

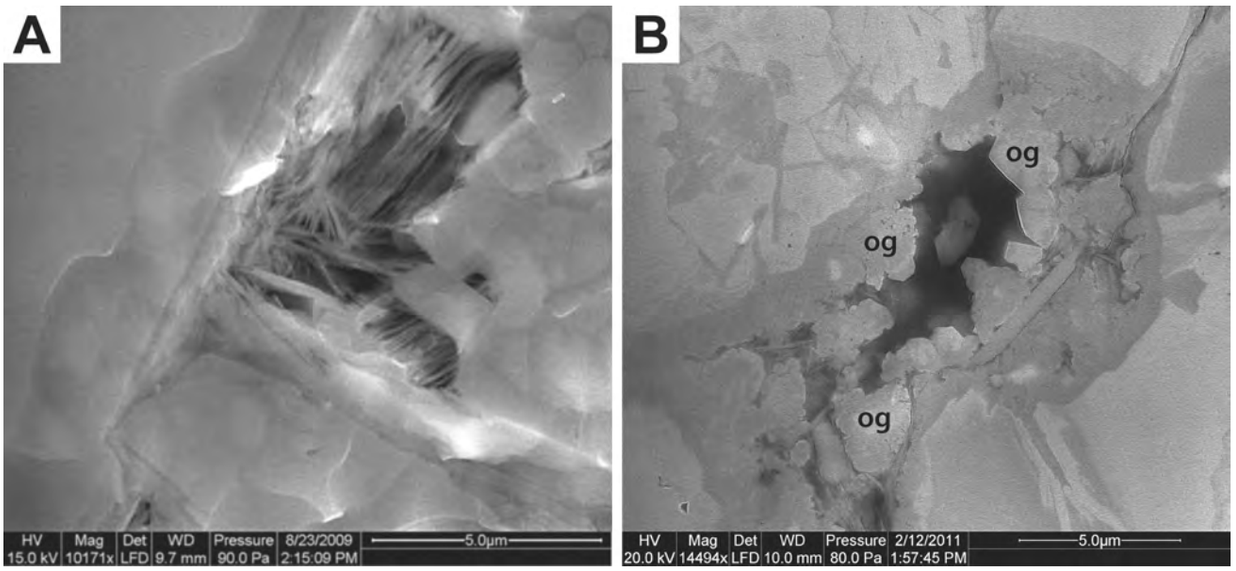

Figure 4. (A) A framework pore between dolomite grains that is partially filled with clay minerals. The clays form frameworks and define pores (total organic carbon [TOC] approximately 5%). (B) Amorphous organic matter (OM) (black) fills intergranular pore partially lined by quartz overgrowths (og) between quartz silt grains (q). Note lack of OM pores in this low-maturity ($<0.6\%R_o$) sample (TOC approximately 10%). Scanning electron microscopic (SEM) secondary electron images from the New Albany Shale.

Whereas pressure shadows are most helpful for preserving phyllosilicate framework pores, clay mineral clamping and pore propping by diagenetic minerals can also provide protection from compactional closure. Clamping of clay platelets in the margins of expanding diagenetic minerals effectively cements phyllosilicate frameworks in place and protects them from compactional collapse (Figures 6B, C, D). Likewise, diagenetic mineral grains can prop open triangular spaces between clay platelets and thus prevent their collapse during compaction (Figures 7A, B, C).

Dissolution pores are commonly observed when carbonate grains (typically dolomite and calcite) are scattered through the shale matrix, or where carbonate grains have been reworked into thin lag deposits. Dissolution rarely removes entire grains (Figure 7A). More commonly, partial dissolution is observed along the carbonate grain margins, resulting in corroded seams and generally vuggy (honeycombed) carbonate minerals (Figures 6B, C). These corroded seams range in width from a few tens to several hundreds of nanometers. Dissolution pores are either irregular in shape or retain rectangular outlines because of the structure of the carbonate substrate (Figure 6D). In charge contrast imaging and under cathodoluminescence, many carbonate grains show zonation that reflects variable contents of magnesium and iron in these grains, as verified by energy-dispersive spectrometry (EDS). No signs of collapse into aforementioned dissolution cavities have been observed, and they do not appear to be filled with secondary minerals. The described style of carbonate dissolution is a common type of secondary porosity in the New Albany Shale. Dissolution features were also observed in association with pyrite grains (Figure 7), but appear much rarer than carbonate dissolution.

The organic matter observed in the New Albany core was largely composed of two types of kerogen: structured organic matter and amorphous organic matter. Structured organic matter retains the morphologic features of the originating organism (e.g., alginites such as *Tasmanites* cysts) (Figures 8A, B). *Tasmanites*, the cyst stage of fossil marine algae, is abundant in eastern U.S. black shale beds and is the most readily identified variety of structured organic matter throughout the Devonian. When examined with epifluorescence microscopy (UV light), *Tasmanites* will fluoresce bright yellow in immature samples, whereas the interstitial amorphous (unstructured) organic matter will produce a dull brownish fluorescence color, a typical UV response for this type of maceral (Taylor et al., 1998). Amorphous organic matter occurs as discontinuous laminae and irregular patches that fill spaces between mineral grains (Figures 7A; 8C, D). The latter form of organic matter is commonly described as amorphinite/bituminite by organic

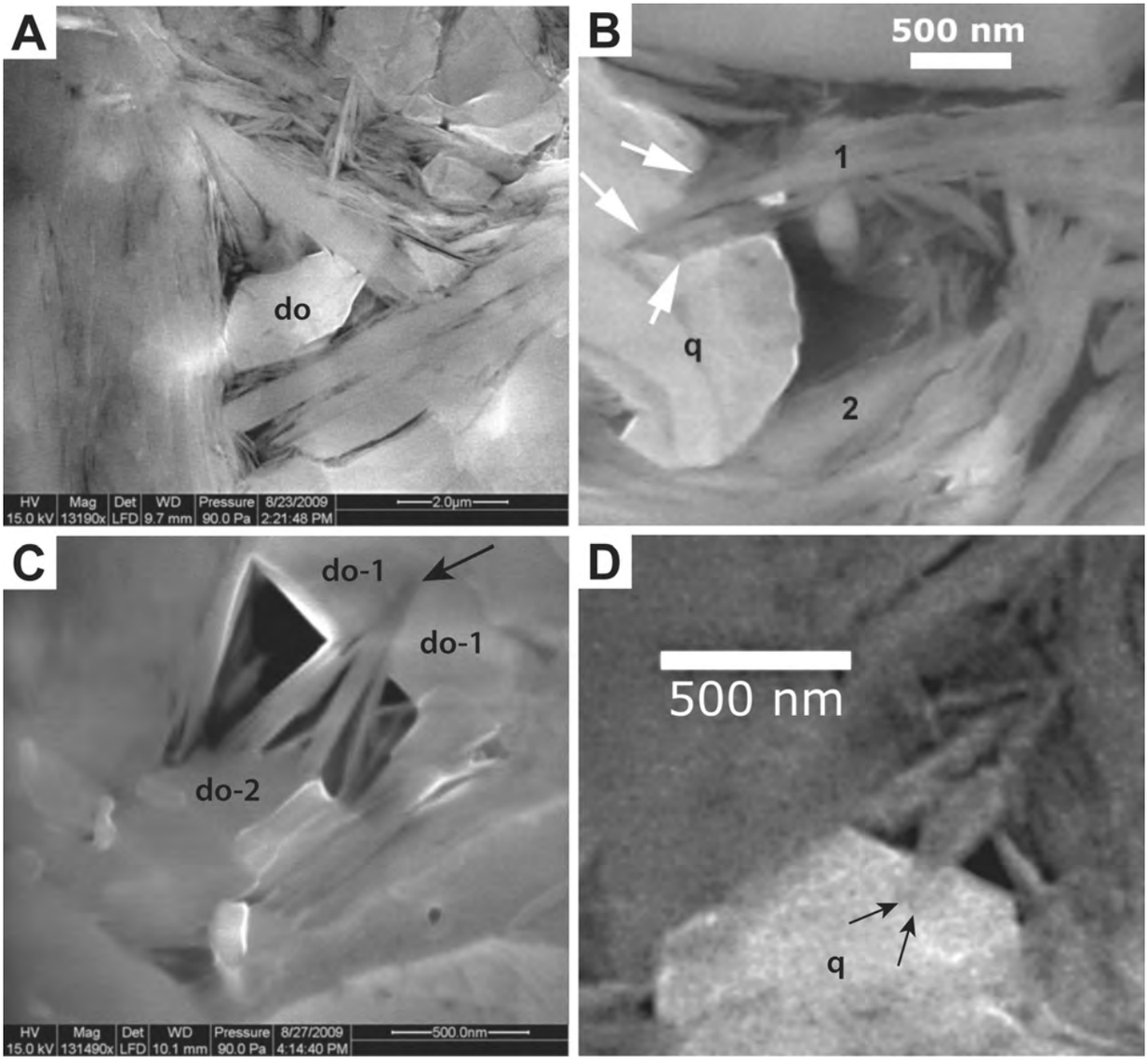

Figure 5. (A) Triangular phyllosilicate framework pores. Dolomite grain (do) partially fills and props open a space between clay platelets. (B) Close-up from Figure 2F shows phyllosilicate framework and an authigenic quartz grain (q). Clay platelet marked 1 has been clamped in place by the growing quartz grain (arrows). The authigenic quartz clamps clay platelets and props open pore spaces. (C) Clamping and propping by authigenic dolomite. Dolomite grain marked do-1 clamps clay platelets (arrow) in place, and dolomite grain marked do-2 props open pore space. (D) Clamping of clay platelet (arrow) by authigenic quartz grain (q). Scanning electron microscopic (SEM) secondary electron images from the New Albany Shale. Total organic carbon (TOC) values for these samples were in the 3 to 5% range.

petrographers (Taylor et al., 1998) and is considered to represent bacterially degraded marine organic matter (phytoplankton, zooplankton). In the thermally immature New Albany Shale, both organic matter categories (structured vs. amorphous) develop smooth ion-milled surfaces and lack pores that are visible at the image resolution of a field emission SEM.

MARCELLUS SHALE

Overview

Samples from a 90 m (295 ft) thick Marcellus core (Beaver Meadow 1 well, Chenango County, New York) were provided by Taury Smith of the New York

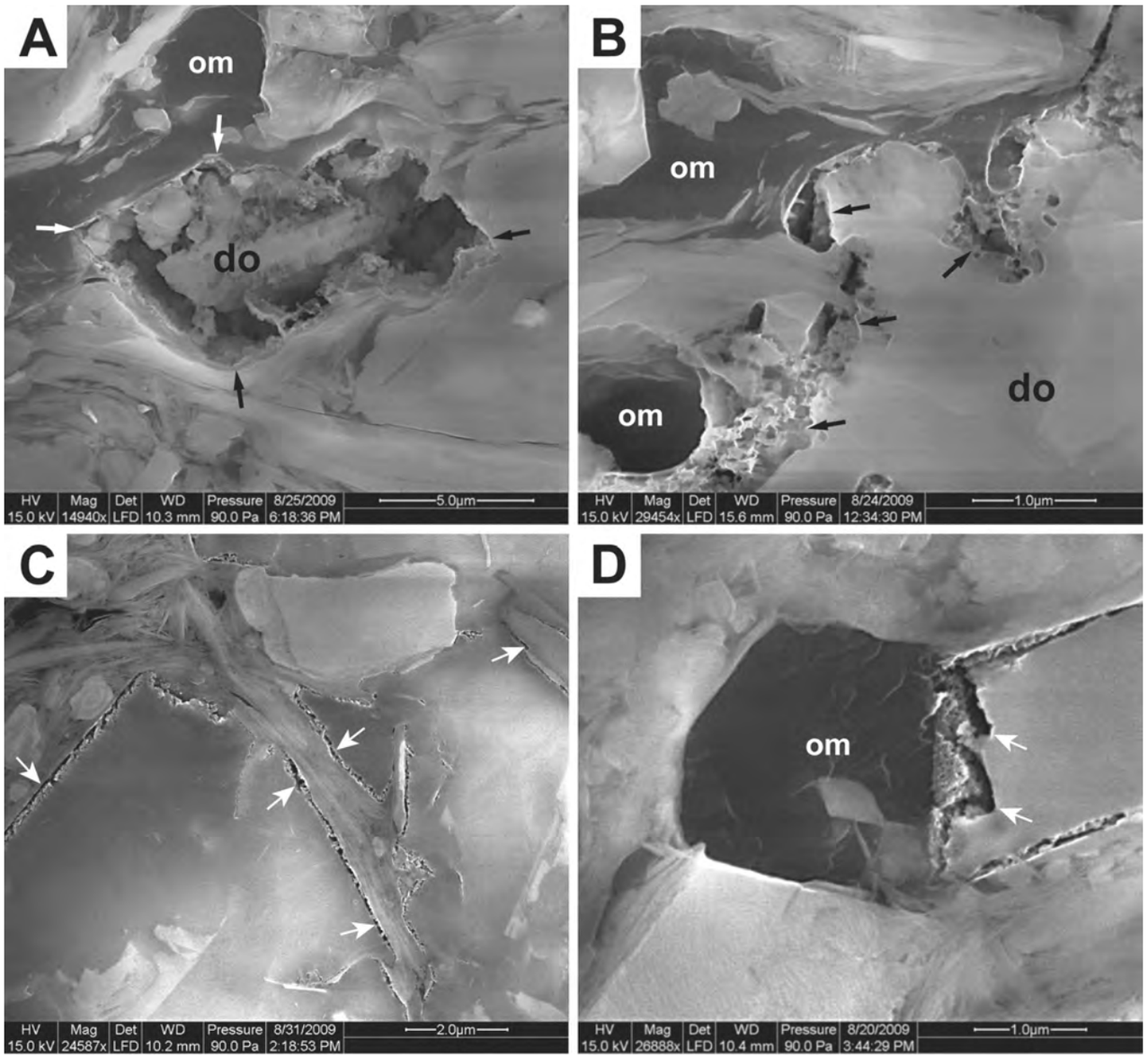

Figure 6. Manifestations of carbonate dissolution in the New Albany Shale. (A) A secondary pore caused by partial dissolution of a dolomite (do) grain. The dolomite nature of the residual material in the center was verified with energy-dispersive spectrometry (EDS) analysis. Pore margins marked by white and black arrows; nonporous organic matter marked om. (B) Corrosion and porosity formation (arrows) along the margins of a dolomite grain. Nonporous organic matter marked om. (C) Dissolution along margins of dolomite grains. Arrows point to dissolution porosity. (D) Dolomite grain margin etched along crystallographic boundaries (arrows), as well as honeycombed dolomite. Nonporous organic matter fills pore. Scanning electron microscopic (SEM) secondary electron images from the New Albany Shale. Total organic carbon (TOC) values for these samples were in the 8 to 9% range.

State Museum (see Table 1 for stratigraphic position and member of samples). Stratigraphic subdivisions present in the core include (in ascending order) the Union Springs Member, the Cherry Valley Limestone, and the Oatka Creek Member (T. Smith, 2010, personal communication). A total of five samples, spanning the 566.9 to 591.3 m (1860 to 1940 ft) depth interval, were examined. Measured vitrinite reflectance values show the Marcellus to be gas mature (2.1%R_o, Weary et al., 200).

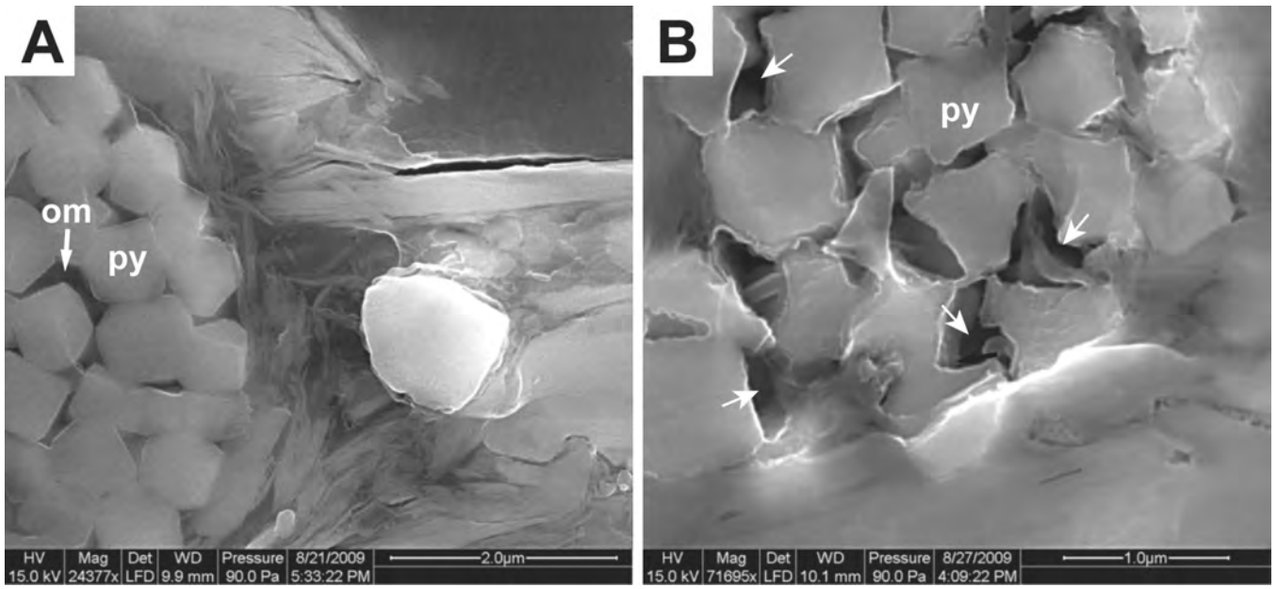

Figure 7. Secondary electron scanning electron microscopic (SEM) images showing manifestations of pyrite dissolution in the New Albany Shale. (A) The left third of the image consists of a pyrite framboid that shows an infill of organic matter (om) between pyrite (py) crystallites. This is very typical for pyrite framboids in the New Albany and many other Devonian black shales. Note also that the framework pores of clays in the central portion of the image are filled with nonporous amorphous kerogen, a typical feature of immature ($<0.6\%R_o$) New Albany samples. The horizontal pore in the upper-right quadrant of the image, at the boundary between dark organic matter and clay mineral flake, is an artifact caused by sample expansion. (B) Close-up of pyrite framboid where pyrite crystallites have undergone corrosion along margins and secondary pores (arrows) are visible between pyrite crystallites. Total organic carbon (TOC) values for samples were approximately 8% (A) and 3% (B).

The shale matrix in the Marcellus Shale consists of a mixture of clay minerals (dominantly illite, Figure 9), quartz grains, carbonate grains (dolomite and calcite), and organic matter. The latter consists of structured kerogen (retaining original structures and outlines) and unstructured kerogen that fills interstitial spaces between mineral grains. Some of the intervals sampled include common to abundant calcareous shell debris derived from ostracods, tentaculites (styliolinids), and small brachiopods (Figure 10).

Observations

Framework pores defined by phyllosilicate grains are ubiquitous in the Marcellus Shale (Figure 9) and consist of triangular openings defined by a latticework of randomly oriented clay mineral platelets (Figure 9). These triangular pores range in size from 10 nm to more than a micrometer and tend to be best developed in areas that were protected from the full force of compactional pressures. Protected areas occur in pressure shadows adjacent to larger compaction-resistant, rigid grains.

In beds and laminae with calcareous shell material, interior cavities of fossils provided shelter from compaction (Figure 10B). The shale matrix within such cavities shows abundant uncollapsed phyllosilicate frameworks with preserved pores (Figures 10C, D). That fossil cavities stayed open for some time during shale burial is indicated by calcite infills (Figure 10A), and whereas true shelter porosity was not seen in the studied samples, it is likely to occur elsewhere in the Marcellus Shale.

In the examined Marcellus samples, carbonate grains and authigenic cements are common features. Preservation of framework pores between carbonate grains is widespread, and these pores range from several hundred nanometers to more than a micrometer in size (Figures 11A, B, C). The carbonate grains appear to have facilitated preservation of phyllosilicate frameworks within carbonate-rich bedsets and laminae. Clay mineral clamping and pore propping by carbonate minerals (Figure 9C, D, E, F) is commonly observed

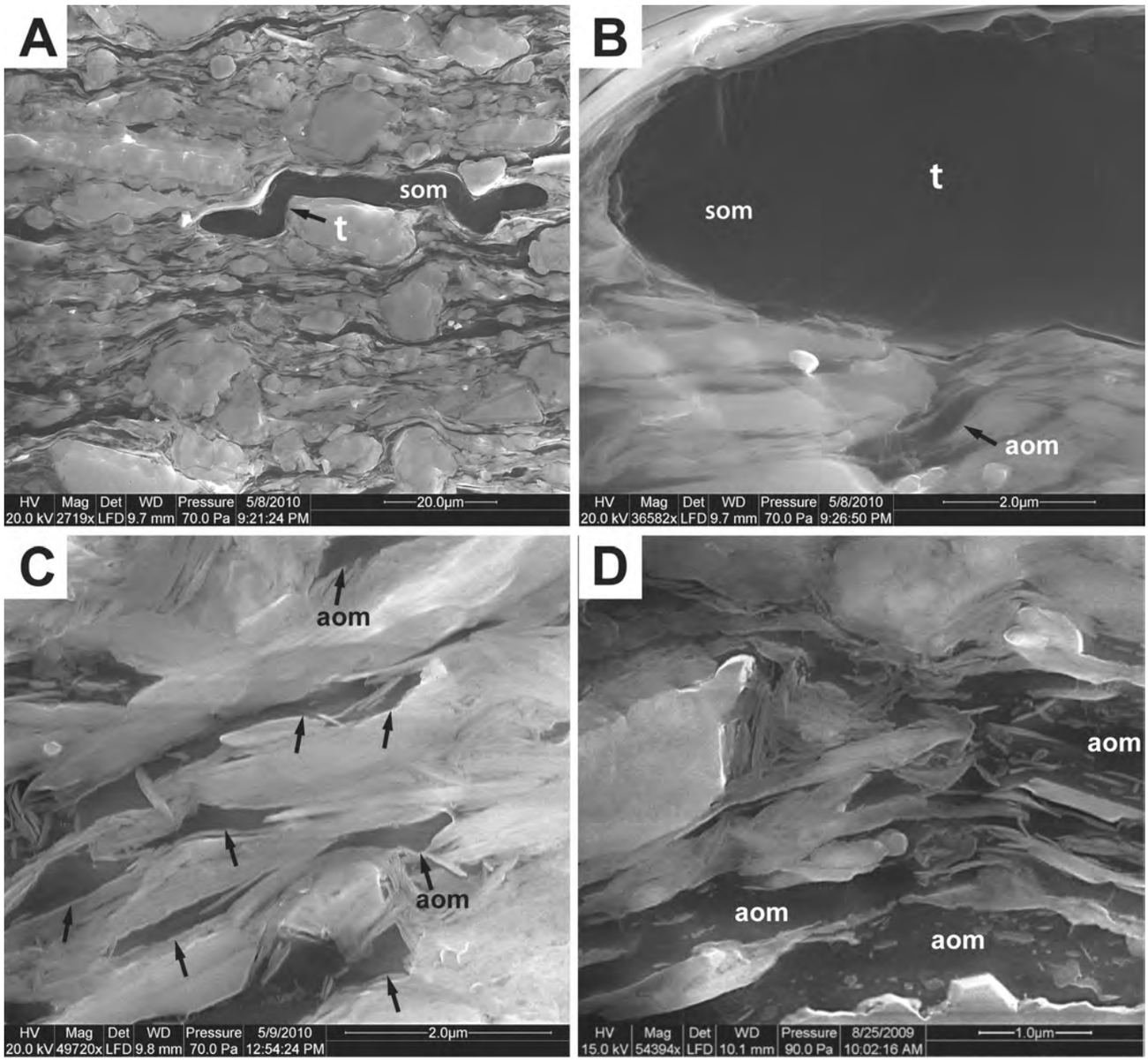

Figure 8. Secondary electron scanning electron microscopic (SEM) images of immature ($<0.6\%R_o$) New Albany Shale. (A), (B) The object t is a collapsed *Tasmanites* cyst. The ion-milled surface of this structured kerogen maceral (som) is smooth and shows no visible pores at maximum SEM magnification. Under ultraviolet (UV) light, the *Tasmanites* macerals exhibit bright yellow fluorescence, consistent with the low thermal maturity. Nonstructured or amorphous organic matter (aom) is also present. (C), (D) Amorphous organic matter is intimately mingled with mineral matter. This amorphous kerogen also shows a smooth ion-milled surface, lacks visible pores, and has a dull brownish fluorescence under UV light. Total organic carbon (TOC) values for these samples were in the 8 to 10% range.

in the Marcellus Shale. In samples where authigenic silica cement is abundant (Figure 11D), it parallels the effects of carbonate cementation, and helps to preserve phyllosilicate frameworks from compactional collapse, as well as defining interstitial pores.

Dissolved margins (Figures 11E, F) were observed on carbonate grains but were uncommon. Their presence suggests late diagenetic dissolution effects associated with organic acids (phenolic and carboxylic acids). Because the lower members of the Marcellus

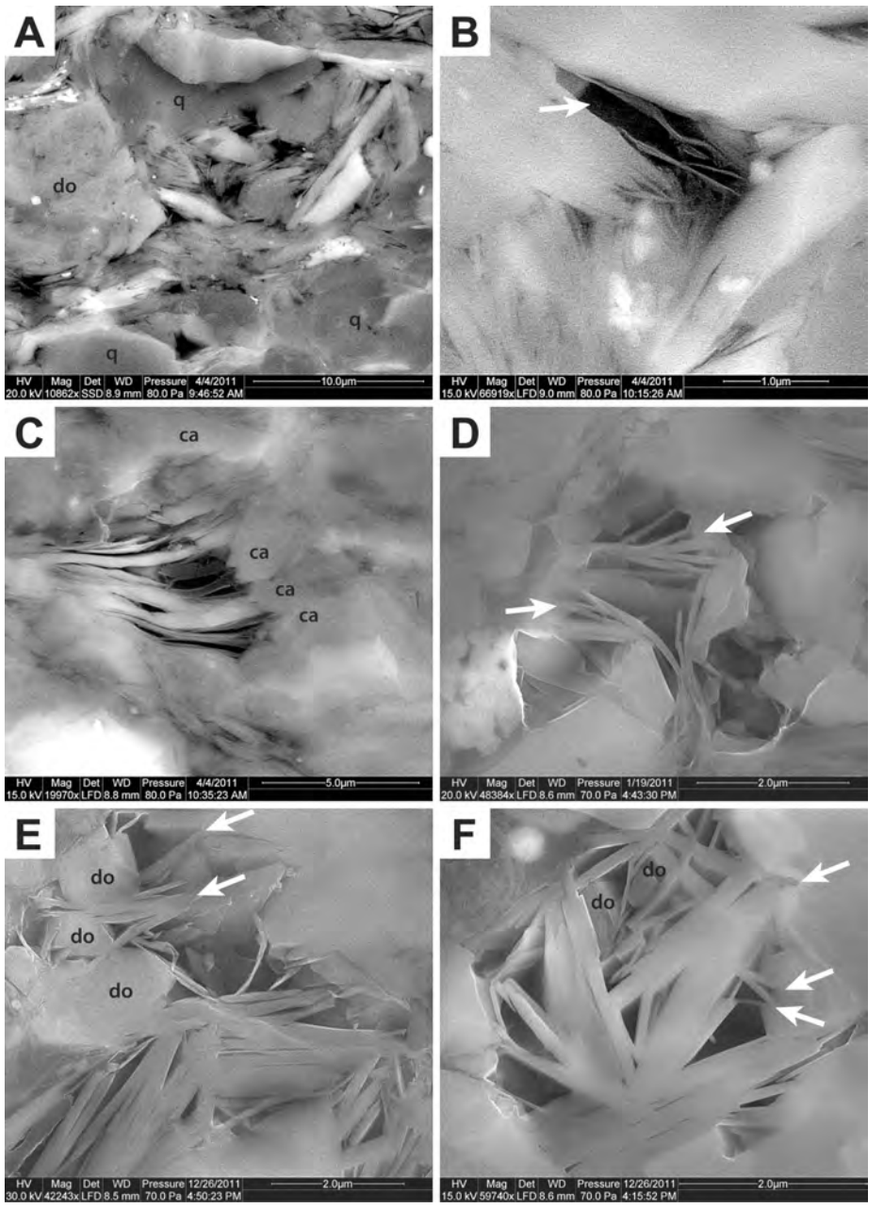

Figure 9. Fabric and phyllosilicate framework pores in samples from the Marcellus Shale. (A) Backscattered electron scanning electron microscopic (SEM) image showing shale matrix consisting of quartz silt grains (q), dolomite grains (do), and clay mineral flakes. Note framework texture of clay flakes in central portion of image. (B) Close-up of large pore (arrow) in framework texture defined by clay minerals (illite). (C) In center of image, clay mineral flakes with intervening pores. To the right (arrows), the pores have been prevented from collapsing by authigenic calcite grains (ca) that propped open the pore space and clamped the clay flakes in place. (D) Phyllosilicate framework and clamping of clay mineral flakes (arrows). (E) Phyllosilicate framework with propping of pores by diagenetic dolomite (do) and clamping of clay mineral in diagenetic carbonate (arrows). (F) Phyllosilicate framework with triangular pores. Some pores propped by diagenetic dolomite. Also, some clay flakes clamped by diagenetic carbonate. (B)–(F) Secondary electron SEM images.

Shale, as well as the lower portion of the Oatka Creek Member, are carbonate rich (unpublished data, L.B. Smith), the system was well buffered against strong pH excursions (unlike the generally carbonate-poor New Albany Shale). Thus, this type of dissolution feature may be a localized phenomenon. Carbonate dissolution pores may be more prevalent in other areas of the basin.

Pores in organic matter (organic matter pores) occur in all samples and are restricted to the unstructured, amorphous organic matter. Amorphous organic matter may include material that was partially degraded by microbes (Pacton et al., 2011), is disseminated throughout the rock matrix, and also fills open spaces in fossil cavities. Structured kerogen (e.g., remains of marine algae such as *Tasmanites*) is devoid of organic matter pores (Figures 12A, B). Amorphous kerogen contains abundant pores in the thermally mature Marcellus Shale samples (Figure 12C). Two types of pores have been observed within amorphous kerogen: (1) abundant tiny pores in the 10 to 50 nm range (foam pores) and (2) a superimposed small population

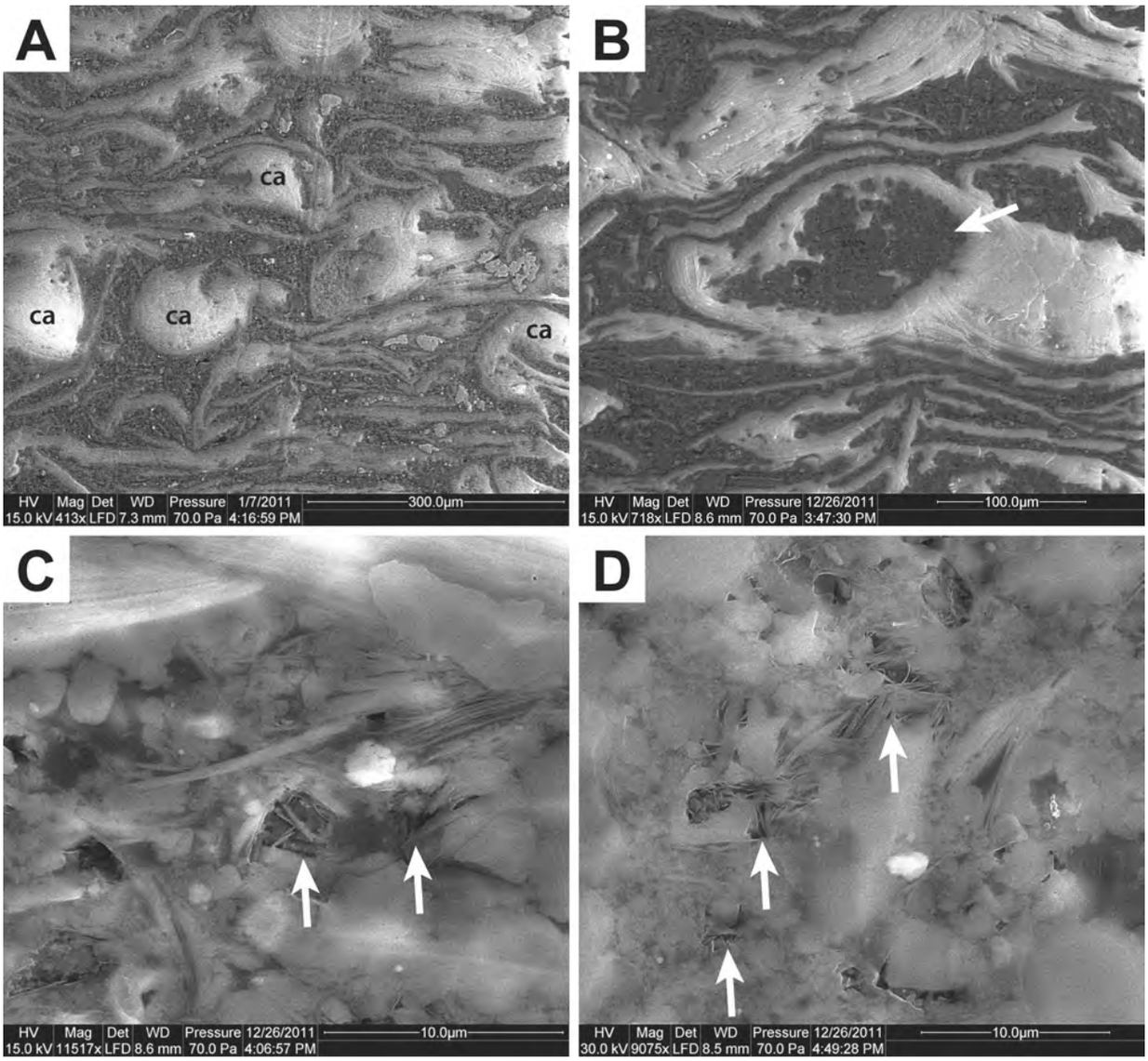

Figure 10. Fossil debris (ostracod shells) shelters framework textures and associated pores from compaction in the Marcellus Shale. (A) Overview secondary electron image with abundant ostracod shells in shale matrix. A number of sheltered spaces are filled with calcite cement (ca). (B) Closer view of a sheltered space (arrow) that is filled with shale matrix. (C), (D) Close-ups of sheltered space from image (C). Arrows point to areas with preserved phyllosilicate framework textures and preserved porosity.

of larger pores (bubble pores) in the 100 to 1000 nm size range (Figures 12D, E, F). Texturally this results in the overall appearance of a sponge. The rounded bubble pores in particular suggest formation in some sort of fluid phase, quite possibly bitumen (Bernard et al., 2012). The close spatial association with foam pores suggests a like origin for these smaller organic matter pores as well. A definite correlation of organic matter pores in the Marcellus with bitumen, however, will require direct confirmation of porous bitumen by other analytical methods (e.g., organic petrography). Nonetheless, the fact that the suspected bitumen areas are typically only a few micrometers in size (Figure 12) makes organic petrographic observations a challenging task. Based on observations of the five Marcellus Shale samples in this study, it appears that organic matter pores may well be the dominant pore type. However, in certain horizons, contributions by phyllosilicate and carbonate-defined frameworks may add to the overall porosity.

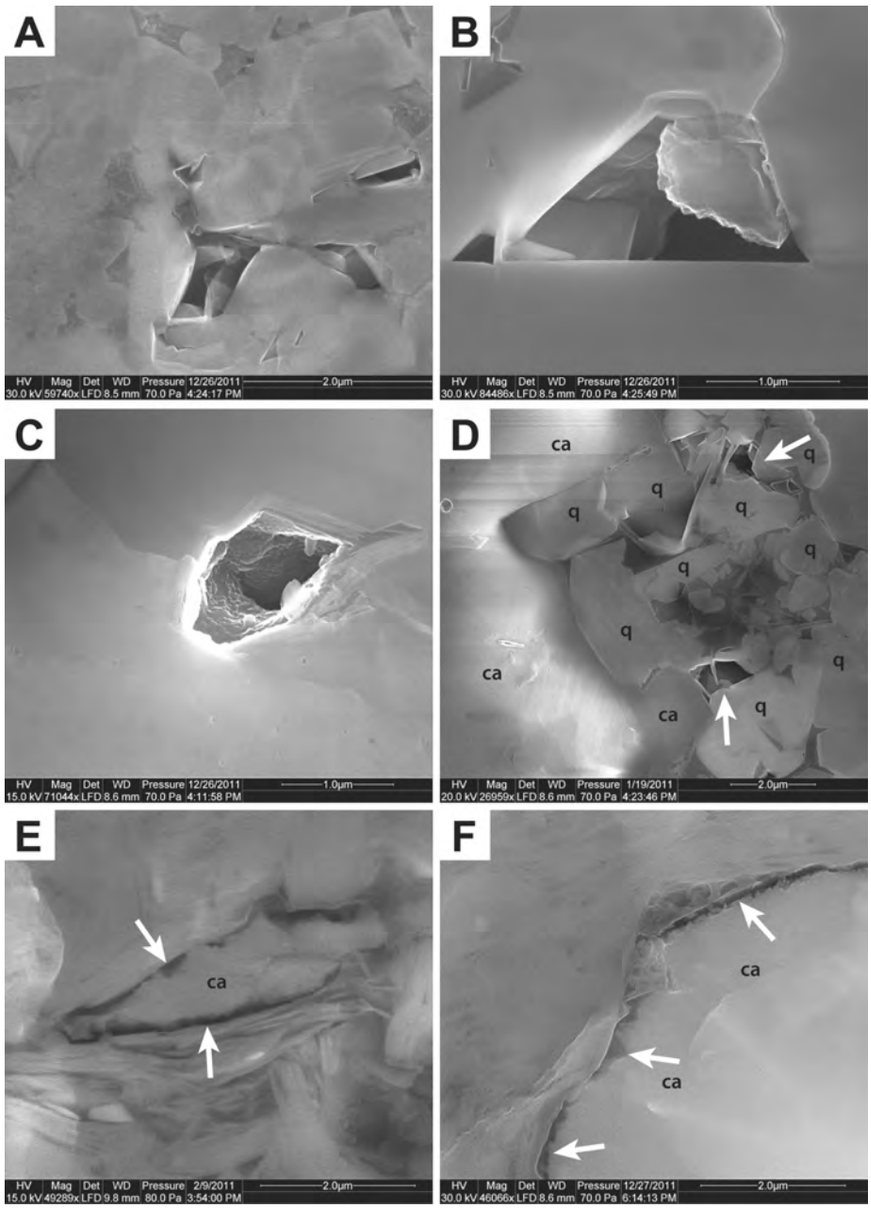

Figure 11. Secondary electron images illustrating pore types in carbonate-rich portions of the Marcellus Shale. (A) Interlocking carbonate grains defining carbonate framework pores. (B) Framework pores bounded by crystal faces of calcite. (C) Framework pore between calcite grains. The dimpled surface in the interior of the pore probably consists of kerogen residues. (D) Calcite grains (ca) surround an area with authigenic quartz (q). Arrows point to pores within quartz grain framework. (E), (F) Carbonate dissolution pores. The rims of calcite grains are partially dissolved (arrows), giving rise to secondary porosity.

DISCUSSION OF PORE OBSERVATIONS

Phyllosilicate framework pores, as illustrated for the New Albany and Marcellus shales, are ubiquitous in many shale successions with an appreciable clay component (Schieber, 2010). These pores have been documented in high-resolution TEM studies of other shale units (e.g., Yau et al., 1987, their figure 2a; Hover et al., 1996, their figure 5). In these earlier studies (Yau et al., 1987; Li et al., 1995; Hover et al., 1996; Rask et al., 1997; Masuada, 2001) the samples were ion milled to a thickness of about 100 to 200 nm, and although the focus was on clay minerals and the smectite-to-illite transformation during burial diagenesis, the pores are clearly visible in published images. Because of the very thin and fragile nature of these TEM samples, however, whether a given triangular opening between clay minerals was a bona fide pore or simply an ion-milling artifact was not easy to assess. Thus, the potential significance of these triangular features, here described as phyllosilicate framework pores, went unrecognized for decades.

Phyllosilicate transformation in the "Zone of Intermediate Burial Diagenesis" (Surdam et al., 1991) has been documented from many sedimentary basins

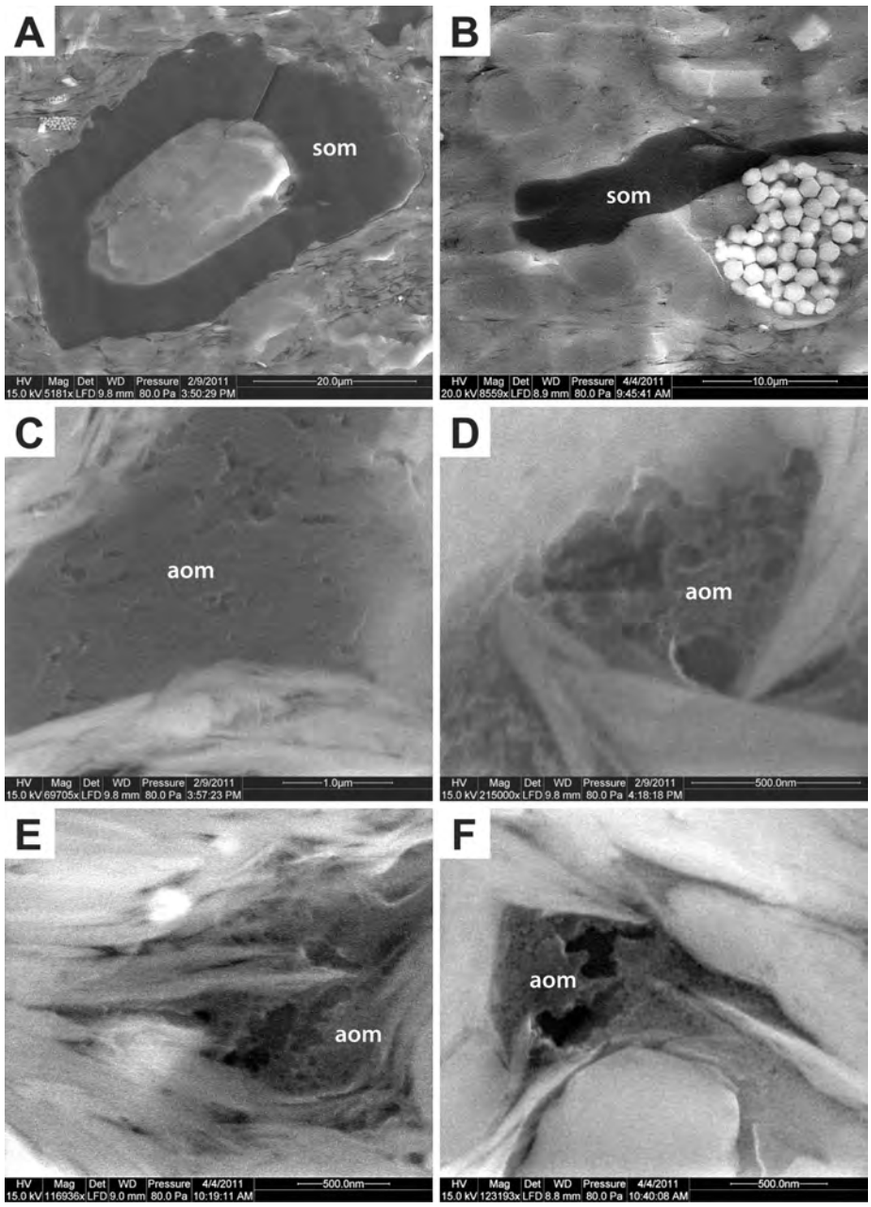

Figure 12. Secondary electron scanning electron microscopic (SEM) images illustrating various forms of organic matter in gas-mature ($>2.0\%R_o$) Marcellus Shale. (A), (B) Structured organic matter (som) in the form of filled (A) and collapsed *Tasmanites* algal cysts (B). The ion-milled surface of this structured kerogen is smooth and shows no visible pores at highest SEM magnification. (C) Interstitial amorphous organic matter (aom). This kerogen material could potentially be bitumen or pyrobitumen and shows pores in the 100 to 500 nm size range. (D) The kerogen/amorphous organic matter (aom) occupies interstitial space between clay minerals. The most abundant pores are in the 20 to 50 nm size range, but a few larger pores in the 100 to 200 nm size range are also present. (E), (F) Kerogen (bitumen?) in interstitial spaces of clay mineral frameworks. In these images, a bimodal pore size distribution is clearly visible. The kerogen groundmass is riddled with small "foam" pores in the 10 to 50 nm size range, and within this foam, larger "bubble" pores that measure 100 to 500 nm in size occur.

and involves the change from smectite to interlayered illite/smectite or to chlorite and/or interlayered chlorite/smectite (e.g., Li et al., 1995; Hover et al., 1996). Contingent on local factors, these phyllosilicate fabrics develop at a burial depth of several kilometers, and the implicit idea has been that they are not predicated by original depositional fabrics. It could thus be argued that phyllosilicate framework pores are to be expected in any shale succession with a sufficient clay content that has been buried deep enough for the onset of the smectite-illite transformation.

In contrast, the observation that phyllosilicate framework pores in the New Albany and Marcellus seem to be associated with lattice frameworks of detrital clay flakes (Figure 3) that imparted partial protection from compaction, and with pressure shadows of compaction-resistant larger grains (Figure 2), suggests that initial depositional fabric leaves a significant imprint on the developing diagenetic fabric parameters. The edge-to-face particle arrangements seen in detrital clay lattice frameworks (Figure 2B) could be a depositional fabric component that reflects

deposition of clays from flocculation. This type of fabric has been observed in other ancient shales and has been attributed to a flocculation origin (e.g., O'Brien et al., 1994). Floccule formation occurs in clay suspensions regardless of salinity (Schieber et al., 2007) and is generally considered a fabric characteristic for clay deposition in a wide range of environments (Bennett et al., 1991). Whereas these initial card-house structures are prone to flattening via compaction (Bennett et al., 1991), partial preservation in pressure shadows, such as illustrated in Figures 2E, F, and 3B, C, D, is to be expected. In fact, next to clays, silt grains of variable composition are the most common component of many shales (Potter et al., 2005), and it is probably not a coincidence that a negative correlation between silt content and seal quality has been observed in other shales (Dawson and Almon, 2002). Observations presented here predict that with increasing silt content there should be an increase in the proportion of "pressure-shadowed" rock volume containing phyllosilicate framework pores. This in turn should translate into an increase in porosity/permeability and result in a decrease of seal quality. Thus, the empirical relationship observed by Dawson and Almon (2002) appears to have a quite rational textural explanation.

The diagenetic dimension of phyllosilicate framework porosity is illustrated in Figure 13. Transmission electron microscopic images from the Cretaceous Mancos Shale (Figures 13A, B, C) show sharply defined triangular pores as small as 10 nm, and mineral growth within these clay mineral defined voids (Figure 13A). The fill is apatite in Figure 13A, but quartz is probably most common, followed by carbonates. The clay platelets in Figures 13A, B, are quite uniform and idiomorphic, and Figure 13C shows thin clay packages with layer terminations in the upper half of the image and clays with a fine-grain felted look in the lower half of the image. All of these features suggest diagenetic growth related to the smectite-illite transformation (e.g., Li et al., 1995; Hover et al., 1996). Although diagenetic cementation can potentially occlude phyllosilicate framework pores, it more typically serves to keep them open either because diagenetic cements act as a proppant or by partially engulfing clay platelets during growth and clamping them in place. Whereas fundamentally any diagenetic mineral can function in this capacity, authigenic carbonates and quartz are most commonly observed.

Because the smectite-to-illite conversion overlaps with the onset of chemical reactions involving kerogens, the latter have a tendency to fill phyllosilicate framework pores. In the New Albany Shale, for example, samples with high TOC values typically show kerogen filling phyllosilicate framework pores (Figure 8). In New Albany samples with comparatively low organic matter contents (e.g., Figure 2), phyllosilicate framework pores have remained open even after deep burial and a long diagenetic history.

Secondary porosity development through corrosion of carbonate grains (Figures 6, 11) implies acidic pore waters and a drop of pH. Research on oil field brines and pore water evolution during burial (e.g., Hayes, 1991; Surdam et al., 1991) suggests that the initial stages of smectite transformation are followed by (and overlap with) decarboxylation of kerogen and a buildup of carboxylic and phenolic acids in

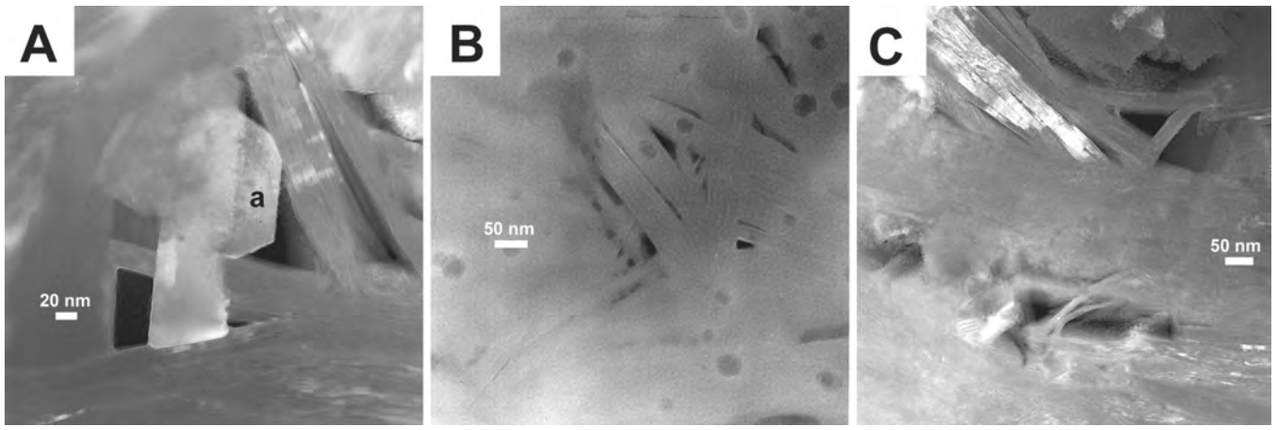

Figure 13. Examples of phyllosilicate framework pores of likely diagenetic origin. All surfaces perpendicular to bedding; images oriented stratigraphic up. (A)–(C) Phyllosilicate framework pores in Mancos Shale (Cretaceous) from the Book Cliffs of Utah. Transmission electron microscopic (TEM) images of samples that were ion milled from both sides. Randomly oriented matrix clays define triangular pores that range in size from 10 to 100 nm. Central pore in (A) is partially filled by diagenetic apatite (marked a).

the temperature range from 80 to 120°C (MacGowan and Surdam, 1990). In sandstones, this stage is associated with formation of secondary porosity (e.g., Hayes, 1991; Surdam et al., 1991) and destruction of carbonates. It seems reasonable to conjecture that the observed carbonate dissolution in the New Albany and Marcellus Shales was likewise linked to organic acid formation. Because the initial amount of organic matter in a shale will place limits on the amount of organic acids that can be generated this way, it seems likely that dissolution porosity of this type is best developed in organic-rich shales. In the overall context, and given that no diagenetic clays were observed in any dissolution cavities, one may conclude that in the studied examples the smectite conversion was largely concluded by the time organic acid production peaked and induced carbonate dissolution.

Because the main phase of hydrocarbon generation and migration follows the formation of diagenetic phyllosilicate frameworks and carbonate dissolution pores (e.g., Hayes, 1991; Surdam et al., 1991), this provides an appealing and logical explanation for the occurrence of amorphous kerogen as well as bitumen, a solid hydrocarbon residue, within phyllosilicate framework pores of thermally mature samples, such as the Marcellus Shale. The amorphous kerogen that occupied pores in the immature New Albany samples may represent an analogous precursor material that would have been present in the immature Marcellus Shale. In the latter, with increasing thermal maturation, the amorphous kerogen may first have converted to bitumen that subsequently developed pores as gaseous hydrocarbons exsolved from the void-filling bitumen. The organic matter pores observed within the gas-mature ($>2.0\%R_o$) Marcellus Shale (Figure 12) are consistent with such a scenario. Because of the higher temperatures required for this step, abundant organic matter pores should only be expected in rocks that have reached sufficient thermal maturity ($>0.6\%R_o$). The observation that well-developed organic matter pores only occurred in the Marcellus Shale samples, a rock unit that has been heated to the dry-gas window ($>2.0\%R_o$; Weary et al., 2000), whereas the similarly organic-rich but immature New Albany Shale ($<0.6\%R_o$; Comer et al., 1994) showed no organic matter pores (Figure 7), supports this assumption. This conclusion is also supported by the work of Loucks and others (2009), who suggested a thermal maturity threshold of greater than $0.7\%R_o$ for the formation of organic matter pores in the Mississippian Barnett Shale of the Fort Worth Basin, Texas. If this reasoning applies broadly, it may also imply that well-developed organic matter porosity (as observed in the Marcellus examples) should occur only within organic-rich (and oil-prone) shales that have reached the gas window or approximately greater than $1.1\%R_o$ (Dow, 1977; Tissot et al., 1987).

In thermally immature rocks, ion-milled amorphous organic material (kerogen) has a smooth appearance, as exhibited by samples from the Devonian New Albany Shale (Figure 8). In rocks that have reached thermal maturity, voids of variable size (a few nanometers to more than a micrometer) are observed in interstitial areas that were once filled by nonporous amorphous kerogen and later converted to bitumen. These were exemplified by samples from the Marcellus Shale (Figure 12). It appears that thermal maturation and migration of hydrocarbons left behind an organic residue that texturally resembles a sponge, consisting of a matrix of organic material with abundant tiny foam pores and superimposed larger bubble pores (Figure 12). The observation that the structured *Tasmanites* kerogen macerals do not exhibit organic matter porosity under the SEM in spite of clearly different levels of thermal maturation between the New Albany (immature) and Marcellus (gas mature) supports the interpretation that organic matter pores are largely restricted to bitumen retained within pore spaces that were filled with amorphous kerogen prior to gas generation.

CONCLUSIONS

Although only two shale units were compared in this study, the pore types illustrated are similar in style to pores that I observed in several other shale units and shale gas reservoirs. Of course, any given shale unit is likely to have unique qualities that affect pore preservation and formation and as such will be different in detail.

Framework, dissolution, and organic matter pore development appear to be an integral part of the depositional, diagenetic, and catagenic history of a given shale succession, particularly the formation of new clay minerals and the maturation of organic matter. It is a well-known fact that freshly deposited modern muds have high water contents, on the order of 80–90% (e.g., Soutar and Crill, 1977; Schimmelmann et al., 1990; Parthenaides, 1991). As water is expelled during burial, the original flocculated fabric collapses and has its best chance of preservation in areas where compaction is minimized by rigid grains (pressure shadows) or within fossil interiors. In addition to this inherited depositional component, phyllosilicate framework pores have a diagenetic component that relates to clay mineral growth during the smectite-to-illite conversion. Phyllosilicate framework pores as described here may be the reason for the observed

correlation between silt content and permeability of other shale units (Dawson and Almon, 2002). To a point, higher clay contents imply more abundant phyllosilicate pores, but high clay contents (50% or more) are probably detrimental because they imply lower silt contents and fewer pressure shadows.

Early diagenetic cements (carbonate, quartz), especially when abundant, can prevent fabric collapse through bridge formation between rigid grains and enable preservation of phyllosilicate frameworks with pores. The presence of these cements may also lead to preservation of open pores between adjacent diagenetic grains.

Secondary carbonate dissolution pores rimming carbonate grains appear to form later in diagenetic history and are probably related to formation of carboxylic and phenolic acids in the course of kerogen maturation. Isolated pores are generated at low carbonate contents, and connected pores may result when carbonate grains are abundant (>10 wt.%) or have been winnowed into laminae.

In shales with high organic matter content (>5 wt.% TOC), framework pores may be initially filled by nonporous organic matter (amorphous kerogen) that may be converted to porous bitumen (pyrobitumen?) at elevated thermal maturity. Shales with lower organic matter content (about 1–5 wt.%) may preserve many of the framework pores in spite of considerable burial and thermal maturation. In the latter instance, framework pores are likely connected and thus potentially able to transmit gas. Void-filling bitumen appears to contain abundant organic matter pores once a shale reaches thermal maturity (>0.6%R_o). The exact relationship between the level of maturity and organic matter pore development is a topic that requires further investigation. Structured kerogen macerals, such as alginite (e.g., *Tasmanites*), do not appear to develop organic matter pores, irrespective of thermal maturity. Whether thermal maturation of structured kerogen indeed does not produce pores or whether the pores are simply too small to be visible at SEM magnifications (<5 nm) is another question that deserves some attention.

Although fracture systems are an important element for shale gas production, at a fracture spacing on the order of decimeters to several meters, gas still has to migrate out of blocks of fracture-bounded shale and into these fractures. Thus, the intrinsic porosity described here is a crucial variable that needs to be understood for a realistic evaluation of long-term production from a given shale unit. The totality of pores in a shale are survivors as well as products of diagenetic and catagenic history, and the described pore types should be a common element in all potential shale gas successions.

Matrix pores as described here represent a key control for gas transfer from the shale matrix to the fractures (natural or artificial) and strongly affect the potential for commercial gas production. Porosity and permeability of shales are a multifaceted topic of considerable economic significance, and this contribution gives a shale petrographer's perspective on pore formation and pore preservation in shales. Petroleum engineers use different methodologies to quantify porosity, such as mercury porosimetry (Thompson et al., 1987) and nitrogen low-pressure isotherm analysis (Sing, 2001). Porosity and permeability data derived by these methods, however, need not necessarily show a close match to independently derived porosity and permeability data because multiple simplifications and assumptions exist (Sing et al., 1985) that fail to do justice to the inherent complexity of fine-grain sediments (Soeder, 1988). Petrographic evaluation of porosity provides an invaluable reality check for these method-driven measurements of porosity and permeability.

ACKNOWLEDGMENTS

I would not have come this far in my work on shale fabrics had it not been for a few lucky coincidences along the way. A bit over two decades ago, David Krinsley provided the initial impetus to incorporate various SEM-based techniques into my research. His enthusiasm was essential at a time when sample preparation techniques still imposed limits on what could be seen via SEM. A decade later, Michael Coviello, a material sciences TEM specialist at UT Arlington, taught me a lot about ion milling samples for electron microscopy. At the same time, Howard Arnott, a UT Arlington biologist, provided access to his well-equipped electron microscopy lab and introduced me to the bag of tricks that biologists use to work with soft and fragile samples. What I learned in these labs has been extremely helpful in developing successful protocols (not all shales are created equal) for ion milling shale samples. More recently, a National Science Foundation (NSF) equipment grant (EAR-0318769) provided funds for the purchase of the analytical SEM (FEI Quanta 400 FEG) that was used for acquiring most of the images used in this contribution. John Rupp of the Indiana Geological Survey and Taury Smith of the New York State Museum were most helpful with providing access to core material and background information about the studied samples. Ion milling and SEM observation of Marcellus Shale samples were generously supported by Malcolm Pirnie Inc. GATAN Inc. loaned a beta model of their Ilion ion mill to the IU Shale Research Lab.

REFERENCES CITED

Bennett, R. H., N. R. O'Brien, and M. H. Hulbert, 1991, Determinants of clay microfabric signatures—Processes and mechanisms, *in* R. H. Bennett, W. R. Bryant, and M. H. Hulbert, eds., Microstructure of fine-grained sediments: New York, Springer-Verlag, p. 5–32.

Bernard, S., B. Horsfield, H. M. Schulz, R. Wirth, A. Schreiber, and N. Sherwood, 2012, Geochemical evolution of organic-rich shales with increasing maturity: A STXM and TEM study of the Posidonia Shale (Lower Toarcian, northern Germany): Marine and Petroleum Geology, v. 31, p. 70–89.

Bollinger, D., and R. Fink, 1980, A new production technique: Ion milling: Solid-State Technology, p. 79–84.

Broadhead, R. F., R. C. Kepferle, and P. E. Potter, 1982, Stratigraphic and sedimentologic controls of gas in shale—Example from Upper Devonian of northern Ohio: AAPG Bulletin, v. 66, p. 10–27.

Coleman, J. L., R. C. Milici, T. A. Cook, R. R. Charpentier, M. Kirschbaum, T. R. Klett, R. M. Pollastro, and C. J. Schenk, 2011, Assessment of undiscovered oil and gas resources of the Devonian Marcellus Shale of the Appalachian Basin province, 2011: USGS Fact Sheet 2011–3092, 2 p.

Comer, J. B., T. Hamilton-Smith, and W. T. Frankie, 1994, Source rock potential, *in* N. R. Hasenmueller and J. B. Comer, eds., Gas potential of the New Albany Shale (Devonian and Mississippian) in the Illinois Basin: Illinois Basin Consortium, Gas Research Institute 92-0391/ Illinois Basin Studies 2, p. 47–54.

Davies, D. K., W. R. Bryant, R. K. Vessell, and P. J. Burkett, 1990, Porosities, permeabilities and microfabrics of Devonian shales, *in* R. H. Bennett, W. R. Bryant, and M. H. Hulbert, eds., Microstructure of fine-grained sediments: From mud to shale: New York, Springer-Verlag, p. 109–119.

Dawson, W., and W. R. Almon, 2002, Top seal potential of Tertiary deep-water shales, Gulf of Mexico: Gulf Coast Association of Geological Societies Transactions, v. 52, p. 167–176.

Dow, W. G., 1977, Kerogen studies and geological interpretations: Journal of Geochemical Exploration, v. 7, p. 79–99.

Hayes, J. B., 1991, Porosity evolution of sandstones related to vitrinite reflectance: Organic Geochemistry, v. 17, p. 117–129.

Hover, V. C., D. R. Peacor, and L. M. Walter, 1996, STEM/ AEM evidence for preservation of burial diagenetic fabrics in Devonian shales: Journal of Sedimentary Research, v. 66, p. 519–530.

Jiang, W.T., D. R. Peacor, and E. J. Essene, 1990, Transmission electron microscopic study of coexisting pyrophyllite and muscovite—Direct evidence for the metastability of illite: Clays and Clay Minerals, v. 38, p. 225–240.

Lazar, O. R., 2007, Redefinition of the New Albany Shale of the Illinois Basin: An integrated stratigraphic, sedimentologic, and geochemical study: unpublished Ph.D. thesis, Indiana University, Bloomington, Indiana, 336 p.

Lazar, O.R., and J. Schieber, 2004, Summary of observations from a 40-meter cored interval of the New Albany Shale in well 1-3 Kavanaugh, Daviess County, Indiana, *in* J. Schieber and O. R. Lazar, eds., Devonian black shales of the eastern U.S: New insights into sedimentology and stratigraphy from the subsurface and outcrops in the Illinois and Appalachian basins: Field Guide for the 2004 Great Lakes Section SEPM Annual Field Conference, Indiana Geological Survey Open File Study 04-05, p. 1–6.

Lineback, J. A., 1970, Stratigraphy of the New Albany Shale in Indiana: State of Indiana, Department of Natural Resources, Geological Survey Bulletin, v. 44, 73 p.

Loucks, R. G., R. M. Reed, S. C. Ruppel, and D. M. Jarvie, 2009, Morphology, genesis, and distribution of nanometer scale pores in siliceous mudstones of the Mississippian Barnett Shale: Journal of Sedimentary Research, v. 79, p. 848–861.

MacGowan, D. B., and R. C. Surdam, 1990, Carboxylic acid anions in formation waters, San Joaquin Basin and Louisiana Gulf Coast, U.S.A—Implications for clastic diagenesis: Applied Geochemistry, v. 5, p. 687–701.

O'Brien, N. R., C. E. Brett, and W. L. Taylor, 1994, Microfabric and taphonomic analysis in determining sedimentary processes in marine mudstones: Example from Silurian of New York: Journal of Sedimentary Research, v. A64, p. 847–852.

Pacton, M., G. E. Gorin, and C. Vasconcelos, 2011, Amorphous organic matter—Experimental data on formation and the role of microbes: Review of Paleobotany and Palynology, v. 166, p. 253–267.

Parthenaides, E., 1991, Effect of bed shear stresses on the deposition and strength of deposited cohesive muds, *in* R. H. Bennett, W. R. Bryant, and M. H. Hulbert, eds., Microstructure of fine-grained sediments: New York, Springer-Verlag, p. 175–183.

Potter, P. E., J. B. Maynard, and P. J. Depetris, 2005, Mud and mudstones: Berlin, Springer-Verlag, 297 p.

Rask, J. H., L. T. Bryndzia, N. R. Braunsdorf, and T. E. Murray, 1997, Smectite illitization in Pliocene-age Gulf of Mexico mudrocks: Clays and Clay Minerals, v. 45, p. 99–109.

Schieber, J., 1998, Deposition of mudstones and shales: Overview, problems, and challenges, *in* J. Schieber, W. Zimmerle, and P. Sethi, eds., Shales and mudstones (vol. 1): Basin studies, sedimentology and paleontology: Stuttgart, Schweizerbart'sche Verlagsbuchhandlung, p. 131–146.

Schieber, J., 2002, Sedimentary pyrite: A window into the microbial past: Geology, v. 30, p. 531–534.

Schieber, J., 2004, SEM and TEM study of silica diagenesis in shales from the Cretaceous Blackhawk Formation, Book Cliffs, Utah: Implications for sealing capacity: AAPG Annual Meeting in Dallas, Abstract Volume, p. A124.

Schieber, J., 2010, Common themes in the formation and preservation of intrinsic porosity in shales and mudstones—Illustrated with examples across the Phanerozoic: Society of Petroleum Engineers Unconventional Gas Conference, February 23–25, 2010, Pittsburgh, Pennsylvania, SPE Paper 132370, 10 p., doi: 10.2118/132370-MS.

Schieber, J., 2011, Shale microfabrics and pore development—An overview with emphasis on the importance of depositional processes, *in* D. A. Leckie and J. E. Barclay, eds.,

Gas shale of the Horn River Basin: Calgary, Canadian Society of Petroleum Geologists, p. 115–119.

Schieber, J., J. B. Southard, and K. G. Thaisen, 2007, Accretion of mudstone beds from migrating floccule ripples: Science, v. 318, p. 1760–1763.

Schimmelmann, A., Lange, C. B., and Berger, W. H., 1990, Climatically controlled marker layers in Santa Barbara basin sediments and fine-scale core-to-core correlation: Limnology and Oceanography, v. 35, p. 165–173.

Shirley, K., 2001, Shale gas exciting again: AAPG Explorer, March, p. 1–4.

Sing, K. S. W., 2001, The use of nitrogen adsorption for the characterization of porous materials: Colloids and Surfaces A: Physicochemical and Engineering Aspects, v. 187–188, p. 3–9.

Sing, K. S. W., D. H. Everett, R. A. W. Haul., L. Moscou, R. A. Pierotti, J. Rouquerol, and T. Siemieniewska, 1985, Reporting physisorption data for gas/solid systems with special reference to the determination of surface area and porosity: Pure and Applied Chemistry, v. 57, p. 603–619.

Soeder, D. J., 1988, Porosity and permeability of eastern Devonian gas shale: SPE Formation Evaluation, vol. 3, no. 2, p. 116–124.

Soutar A., and P. A. Crill, 1977, Sedimentation and climatic patterns in the Santa Barbara Basin during the 19th and 20th centuries: GSA Bulletin, v. 88, p. 1161–1172.

Surdam, R. C., D. B. MacGowan, and T. L. Dunn, 1991, Predictive models for sandstone diagenesis: Organic Geochemistry, v. 17, p. 243–253.

Taylor, G. H., M. Teichmüller, and C. Davis, 1998, Organic petrology: Stuttgart, Gebrüder Borntreager, 704 p.

Thompson, A. H., A. J. Katz, and R. A. Raschke, 1987, Mercury injection in porous media: A resistance devil's staircase with percolation geometry: Physical Review Letters, v. 58, p. 29–32.

Tissot, B. P., R. Pelet, and P. Ungerer, 1987, Thermal history of sedimentary basins, maturation indices, and kinetics of oil and gas generation: AAPG Bulletin, v. 71, p. 1445–1466.

Tomutsa, L., D. Silin, and V. Radmilovic, 2007, Analysis of chalk petrophysical properties by means of submicron-scale pore imaging and modeling: SPE Reservoir Evaluation and Engineering, v. 10, p. 285–293.

Yau, Y. C., D. R. Peacor, and S. D. McDowell, 1987, Smectite-to-illite reactions in Salton Sea shales: A transmission and analytical electron microscopy study: Journal of Sedimentary Petrology, v. 57, p. 335–342.

Weary, D. J., R. T. Ryder, and R. Nyahay, 2000, Thermal maturity patterns (CAI and $\%R_o$) in the Ordovician and Devonian rocks of the Appalachian basin in New York: USGS Open-File Report 00-496, USGS, Reston, Virginia.